Electronic Supplementary Information (ESI)

Ferrocene-modified covalent organic framework for efficient oxygen evolution reaction and CO$_2$ electroreduction

Sheng-Nan Sun, [a] Li-Ling He, [a] Qing Huang, [b] Jiang Liu,*[a] Ya-Qian Lan[a]

[a] School of Chemistry, South China Normal University, Guangzhou, 510006, P. R. China.

[b] College of Materials Science and Engineering Nanjing Forestry University, Nanjing, 210037, P.R. China.

*Corresponding author. E-mail: liuj0828@m.scnu.edu.cn

Experimental Section

Materials and Chemicals

N, N-dimethylformamide (DMF), 1, 2-dichlorobenzene, n-butanol, 1, 4-dioxane, methanol (CH$_3$OH), tetrahydrofuran (THF), and triethylamine (Et$_3$N) were purchased from Shanghai Titan Technology Co., Ltd. Acetic acid was purchased from Adamas-beta Co., Ltd. Potassium hydroxide (KOH) and potassium bicarbonate (KHCO$_3$) were purchased from Shanghai Titan Technology Co., Ltd. Trichloromethane (CHCl$_3$) was obtained from Guangdong Guangshi Regent Technology Co., Ltd. Nickel(II) acetate tetrahydrate (Ni(CH$_3$COO)$_2$•4H$_2$O) was purchased from Alfa-Aesar. Bromoferrocene (Fc-Br) was purchased from Macklin. 5, 10, 15, 20-tetrakis(4-aminophenyl)-21H, 23H-porphine (TAPP) and 2, 5-dihydroxy-1, 4-benzenedicarboxaldehyde (Dha) were purchased from Jilin Chinese Academy of Sciences-Yanshen Technology Co., Ltd. All commercial chemicals were used without further purification.

Synthesis of 5, 10, 15, 20-tetrakis(4-aminophenyl)-21H, 23H-porphine-Ni (Ni-TAPP)

TAPP (500 mg) and Ni(CH$_3$COO)$_2$•4H$_2$O (750 mg) were added to a three-neck round-bottomed flask (500 mL). A mixture of CH$_3$OH (50 mL), CHCl$_3$ (225 mL), and DMF (75 mL) was added to the three-necked round bottom flask under nitrogen and then refluxed at 85 °C for 24 h. After cooling to room temperature, the organic phase was collected by extraction with a large amount of water in a separatory funnel and the

product was obtained by rotary evaporation. Finally, the product was dried under vacuum at 80 °C overnight.

Synthesis of Ni-Tph-COF-OH

According to the reported literature, Ni-Tph-COF-OH was synthesized by Schiff base reaction. Ni-TAPP (32.4 mg) and Dha (14.6 mg) were added to a Pyrex tube, in which 1, 2-dichlorobenzene (1 mL) and n-butanol (1 mL) were added. Sonication was performed for 5 min to obtain a homogeneous mixture. After adding 0.2 mL acetic acid (6 M) to the mixture under shaking, the tube was flash-frozen at 77 K (liquid N_2 bath) and degassed through three freeze-pump-thaw cycles by evacuated through an oil pump and then sealed under vacuum. After warming to room temperature, the glass tubes were heated at 120 °C for 3 days. The precipitate was collected by filtration and washed with THF and CH_3OH until the filtrate was colorless. Afterwards, the powder sample was washed with THF in a Soxhlet extractor for 24 hours. Finally, the product was evacuated at 120 °C under a dynamic vacuum overnight to yield activated samples.

Synthesis of Ni-Tph-COF-Fc

Activated Ni-Tph-COF-OH (30 mg), Fc-Br (24 mg), 1,4-dioxane (20 mL), and Et_3N (20 µL) were added to a 100 mL three-necked round bottom flask. After being purified by nitrogen three times, the mixture was refluxed and stirred at 90 °C for 6 hours. After the reaction cooled to room temperature, the precipitate was collected by filtration and washed with CH_3OH several times. Subsequently, the powder sample was washed with CH_3OH in a Soxhlet extractor for 24 hours. Finally, the product was dried in a vacuum oven at 80 °C overnight.

Synthesis of Tph-COF-OH

The synthesis method of Tph-COF-OH is similar to that of Ni-Tph-COF-OH, except for replacing Ni-TAPP with TAPP.

Synthesis of Tph-COF-Fc

The synthesis method of Tph-COF-Fc is similar to that of Ni-Tph-COF-Fc, except for replacing Ni-TAPP with TAPP.

Synthesis of Ni-Tph-COF-2 and Ni-Tph-COF-3

The synthesis methods of Ni-Tph-COF-Fc-2 and Ni-Tph-COF-Fc-3 are similar to that of Ni-Tph-COF-Fc, except for changing the feed mass of Fc-Br to 12 mg and 48 mg.

Characterizations and instruments

Powder X-ray diffraction (PXRD) spectra of the samples were recorded on a Rigaku SmartLab diffractometer (Japan) equipped with Cu Kα (λ = 1.54060 Å) radiation at 40 kV and 200 mA. Fourier transform infrared spectroscopy (FT-IR) was recorded on a NICOLET iS50 with a scanning range of 4000-400 cm^{-1} using pressed KBr pellets. Under air atmosphere, thermogravimetric analysis (TGA) was performed on the PerkinElmer STA-8000 analyzer by heating from room temperature to 800 °C with a heating rate of 10 °C min^{-1}. X-ray photoelectron spectroscopy (XPS) was measured on a scanning X-ray microprobe (PHI 5000 Verasa, ULAC-PHI, Inc.). The result of the isotope-labeled experiment was analyzed by gas chromatography-mass spectrometry (GC-MS, 7890A and 5875C, Agilent). ^{1}H-NMR was carried out on an AVANCE III 400 M spectrometer (Bruker). Scanning electron microscope (SEM) images were taken on Carl Zeiss (ZEISS Gemini 500, Germany). Transmission electron microscopy (TEM) images and high resolution-transmission electron microscopy (HR-TEM) images were collected on a JEM-2100HR at an accelerating voltage of 200 kV.

Electrochemical measurements

All electrochemical tests of the catalysts including oxygen evolution reaction (OER), CO_2 reduction reaction (CO_2RR), electrochemical impedance spectroscopy (EIS), linear sweep voltammetry (LSV) and cyclic voltammetry (CV) were performed on an electrochemical workstation (SP-150, Bio-Logic) under environmental conditions. An airtight H−type cell was used as the reactor, with two compartments of the electrolyzer separated by a proton exchange membrane (Nafion®117, dupont). Each compartment contained 25 mL of electrolyte and left about 25 mL of headspace (1 M

aqueous KOH for OER and 0.5 M aqueous $KHCO_3$ for CO_2RR). Catalyst-modified carbon paper (CP, 1 cm × 2 cm), Ag/AgCl (with saturated KCl), and carbon rods were used as a working electrode, a reference electrode, and a counter electrode, respectively. All potentials in this work, if not specifically accounted for, are described in the data according to the Nernst equation: E (*vs*. RHE) = E (*vs*. Ag/AgCl) + 0.197 V + 0.0592 × pH converted to a relationship with the reversible hydrogen electrode (RHE), and all electrochemical tests were performed without iR compensation.

In the OER experiment, Ar (99.999%) was first passed into the electrolyte and bubbled for more than 30 min to ensure that the electrolyte was saturated with Ar. Subsequently, LSV was performed at a sweep rate of 5 mV s^{-1} under an Ar atmosphere. The Tafel slope was calculated from the LSV based on the Tafel equation: η = blogj + a.

The double-layer capacitance (C_{dl}) was evaluated by CV. CV were performed with different scan rates: 20 mV s^{-1}, 40 mV s^{-1}, 60 mV s^{-1}, 80 mV s^{-1}, 100 mV s^{-1}, 120 mV s^{-1}, and 140 mV s^{-1} in the range of non-Faraday potentials from 0 V to 0.1 V *vs*. Ag/AgCl. The Δ*j* at potential 0.05 V *vs*. Ag/AgCl was plotted relative to the scan rate, and its linear slope was C_{dl}. ECSA was proportional to the C_{dl} value.

In the CO_2RR experiments, Ar (99.999%) was first passed into the electrolyte and bubbled for more than 30 min to ensure that the electrolyte was saturated with inert gas, and the LSV was performed at a sweep rate of 5 mV s^{-1}. Subsequently, the LSV curve was recorded at a sweep rate of 5 mV s^{-1} after bubbling with CO_2 (99.999%) for at least 30 min to saturate the electrolyte with CO_2. Electrocatalytic CO_2RR measurements were performed on an electrochemical workstation by chronocoulometry.

The EIS was measured at a potential of 1.6 V with a frequency range of 1000 kHz to 0.1 Hz using an AC voltage with 10 mV mplitude.

Preparation of working electrodes

The sample (10 mg) and AB (10 mg) were mixed in a mortar for grinding. Then

the evenly ground mixture was transferred to a 2 mL sample tube and 1 mL of a mixed solution containing ethanol (500 μL), water (400 μL), and Nafion (5 wt%, 100 μL) was added to it. The mixture was sonicated for 30 minutes to form a uniform black suspension. Then, the suspension was directly dropped onto CP (1 x 2 cm), with a coating area of 1 x 1 cm^2 and a catalyst loading density of approximately 1 mg cm^{-2}.

Product detection and calculation

The gas-phase reduction products of CO_2RR were detected by gas chromatography (GC, Agilent 7820A) equipped with a flame ionization detector (FID) and thermal conductivity (TCD). The electrolyte after electrolysis was collected from the cathode chamber, and 0.5 mL electrolyte was mixed with 0.1 mL D_2O in a nuclear magnetic tube. The liquid phase products of CO_2RR were analyzed using ^1H-NMR.

For making a standard curve of the gas-phase products of the CO_2 reduction reaction, the procedure was as follows: first 25 mL of electrolyte was added to both the cathode and anode chambers of the H-cell (note that the volume in the cathode chamber contains the magnets used for stirring), and after that, CO_2 was drummed into the electrolyte individually, and it was maintained for at least 30 min in order to saturate it with CO_2. Different amounts of high purity CO were aspirated separately with injection needle, and injected into the cathode chamber with stirring for 20 min, after which a fixed amount of gas was aspirated from the top of the cathode chamber and analyzed by gas chromatography to obtain different data points on the standard curve.

The calculation of faradaic efficiency

For CO,

$$FE = \frac{2F \times n_{co}}{I \times t} \times 100\% \quad \text{(Equation 1)}$$

For H_2,

$$FE = \frac{2F \times n_{H_2}}{I \times t} \times 100\% \qquad \text{(Equation 2)}$$

where F is the Faraday constant (96485 C/mol), n_{co} is the moles of produced CO

and n_{H_2} is the moles of produced H$_2$.
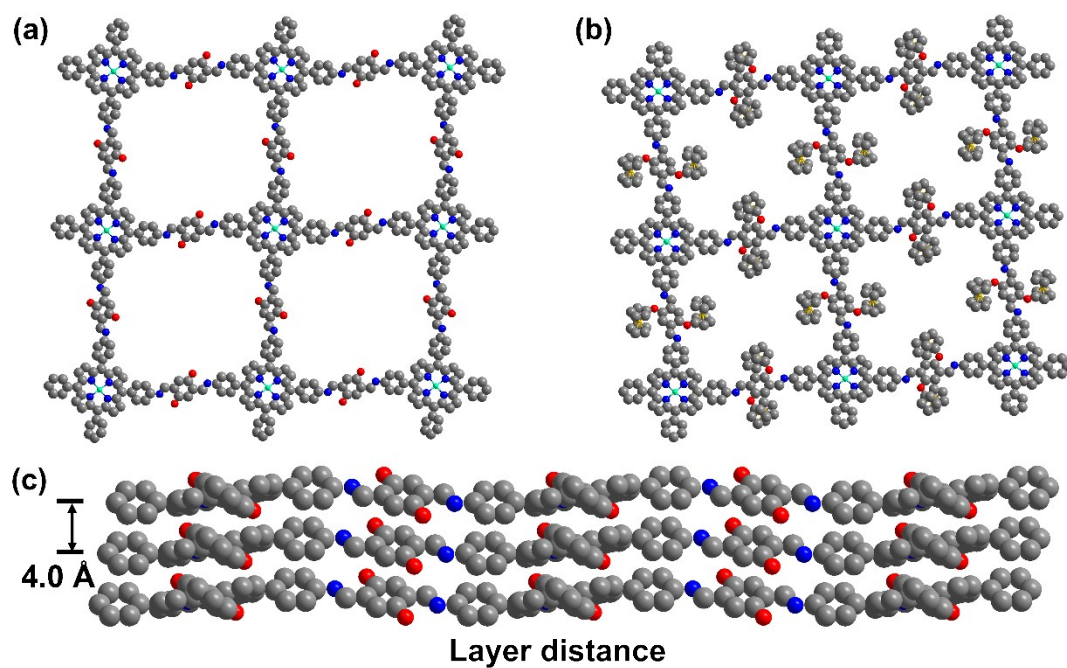
Fig. S1 (a) The structure of Ni-Tph-COF-OH. (b) The structure of Ni-Tph-COF-Fc. (c) The layer distance of Ni-Tph-COF-OH.
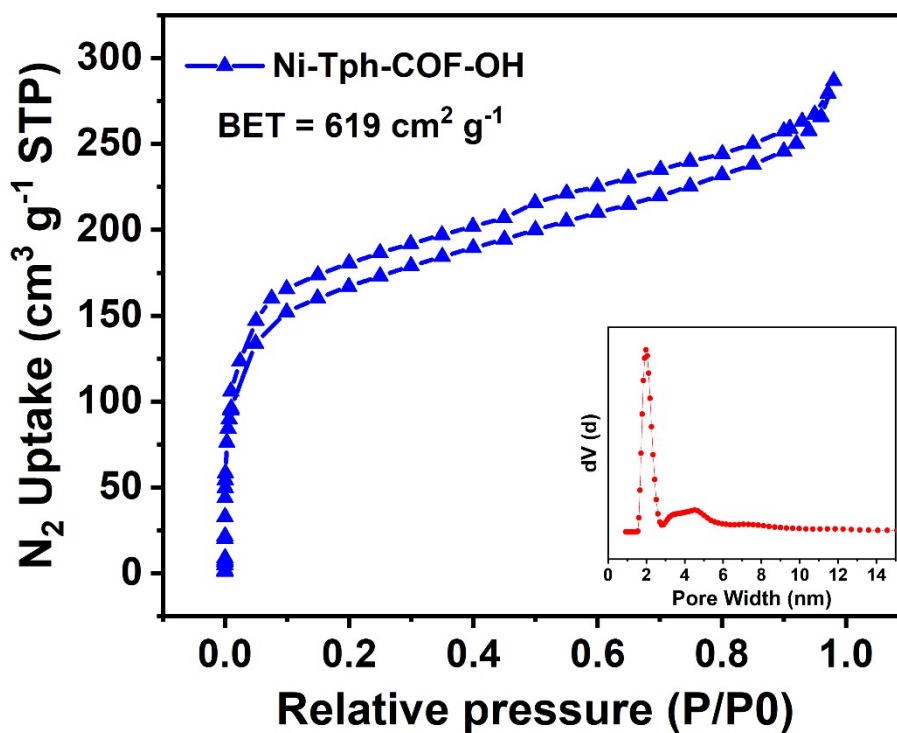
Fig. S2 N_2 sorption isotherms and pore size distribution of Ni-Tph-COF-OH.
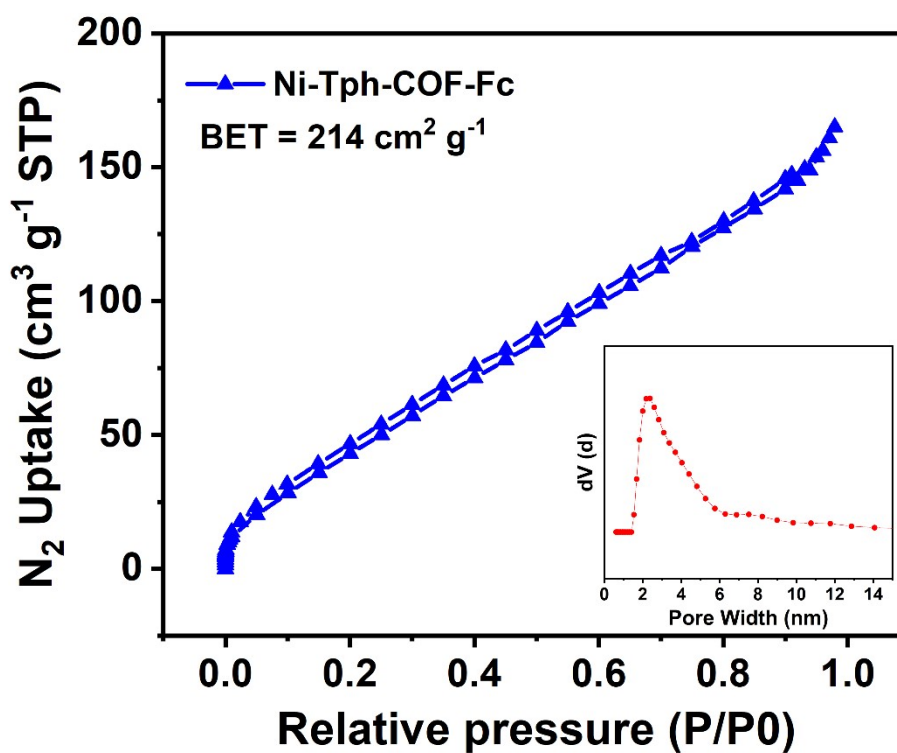
Fig. S3 N_2 sorption isotherms and pore size distribution of Ni-Tph-COF-Fc.
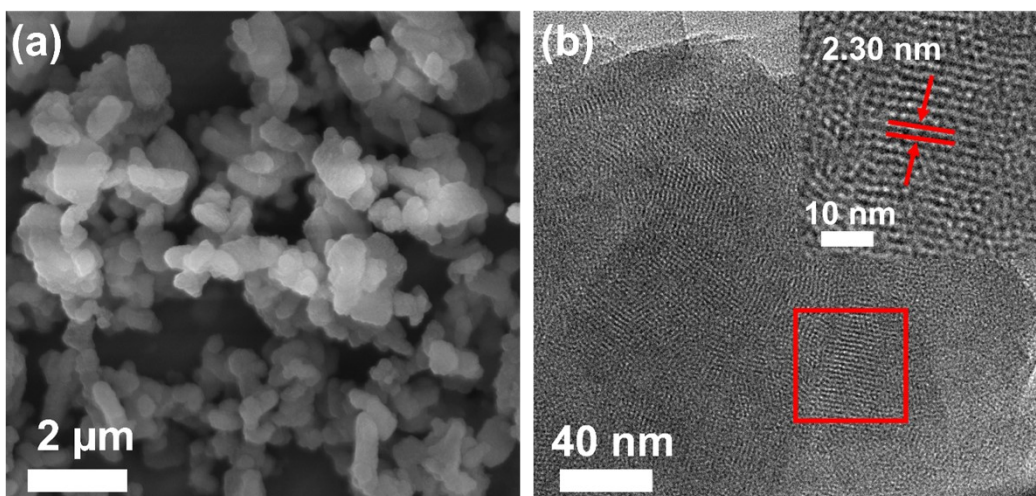
Fig. S4 (a) SEM of Ni-Tph-COF-OH. (b) HR-TEM of Ni-Tph-COF- OH
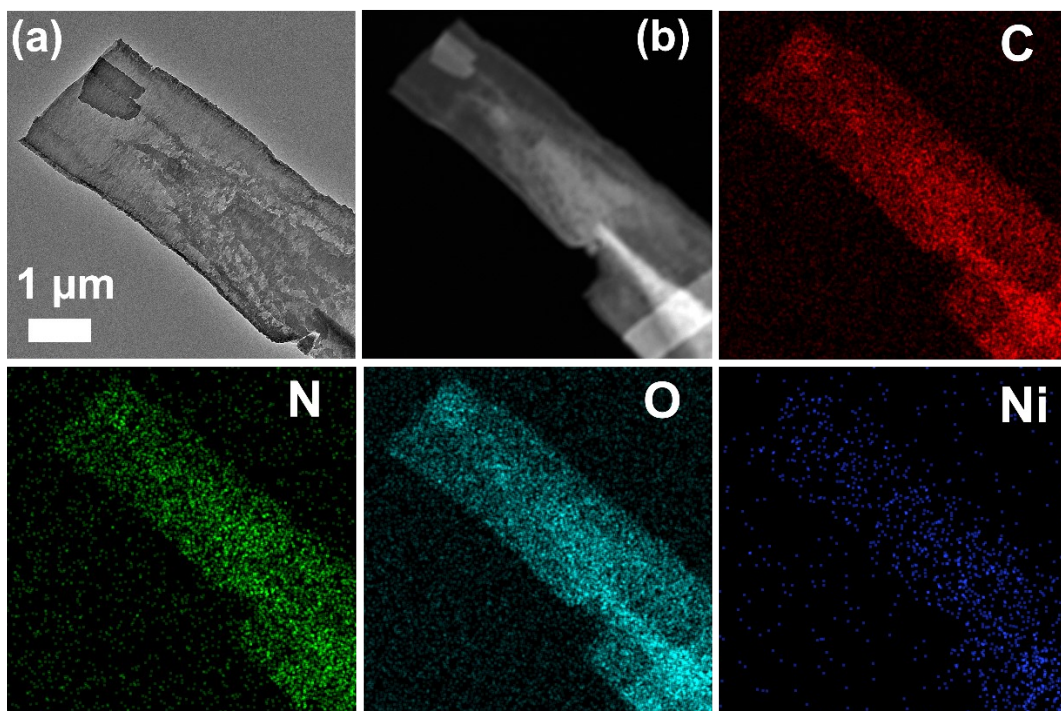
Fig. S5 (a) TEM of Ni-Tph-COF-OH. (b) Mapping of Ni-Tph-COF-OH.
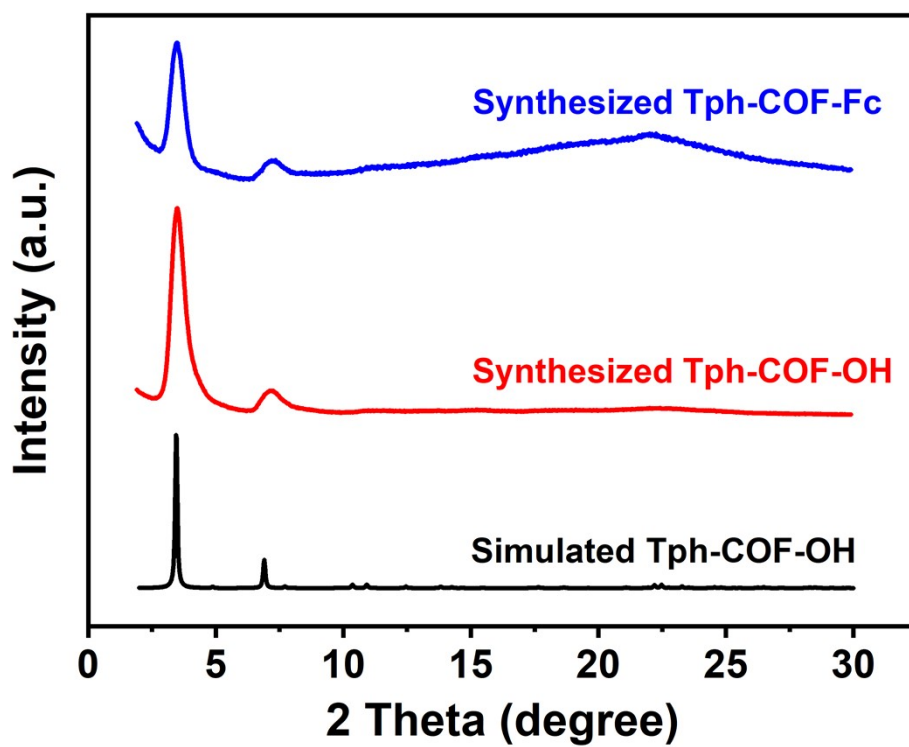
Fig. S6 The PXRD patterns of Tph-COF-OH and Tph-COF-Fc.
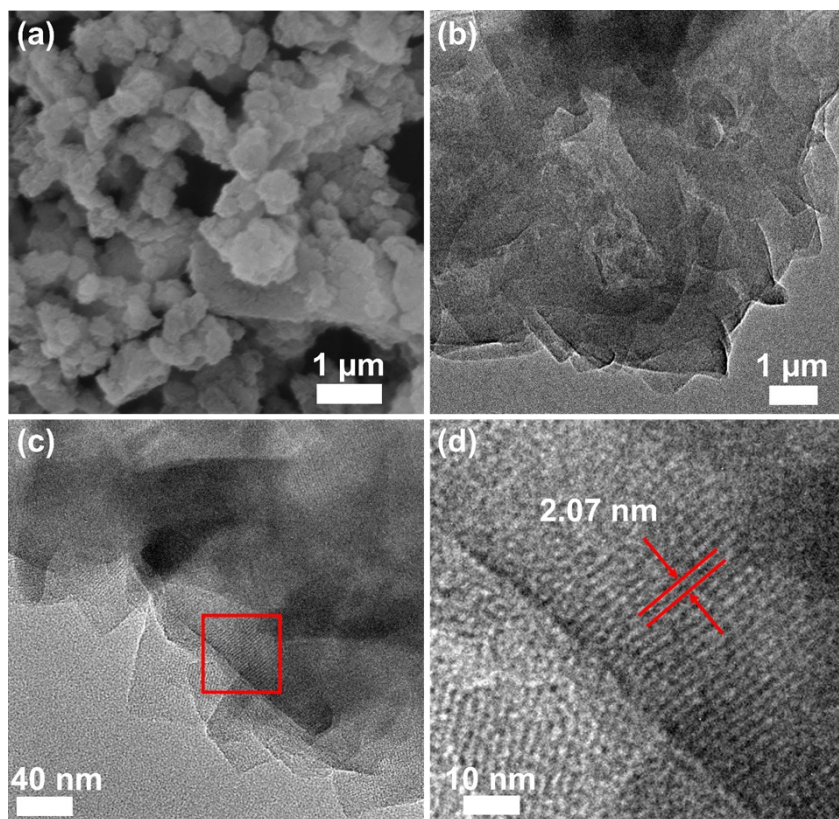
Fig. S7 (a) The SEM image of Tph-COF-OH. (b) The TEM image of Tph-COF-OH. (c, d) The HR-TEM image of Tph-COF-OH.
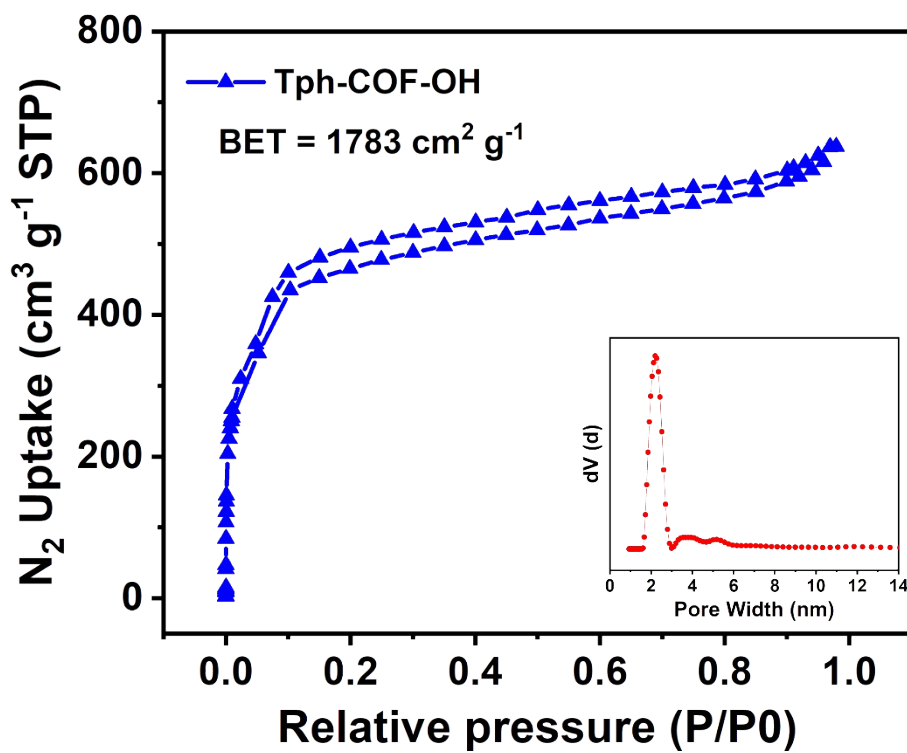
Fig. S8 N_2 sorption isotherms and pore size distribution of Tph-COF-OH.
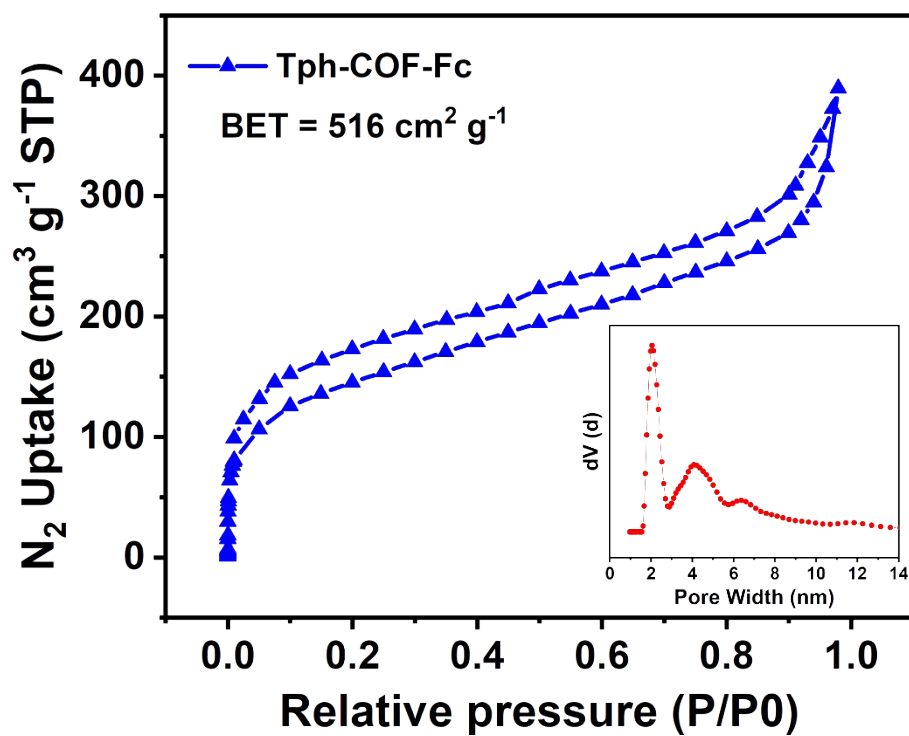
Fig. S9 N_2 sorption isotherms and pore size distribution of Tph-COF-Fc.
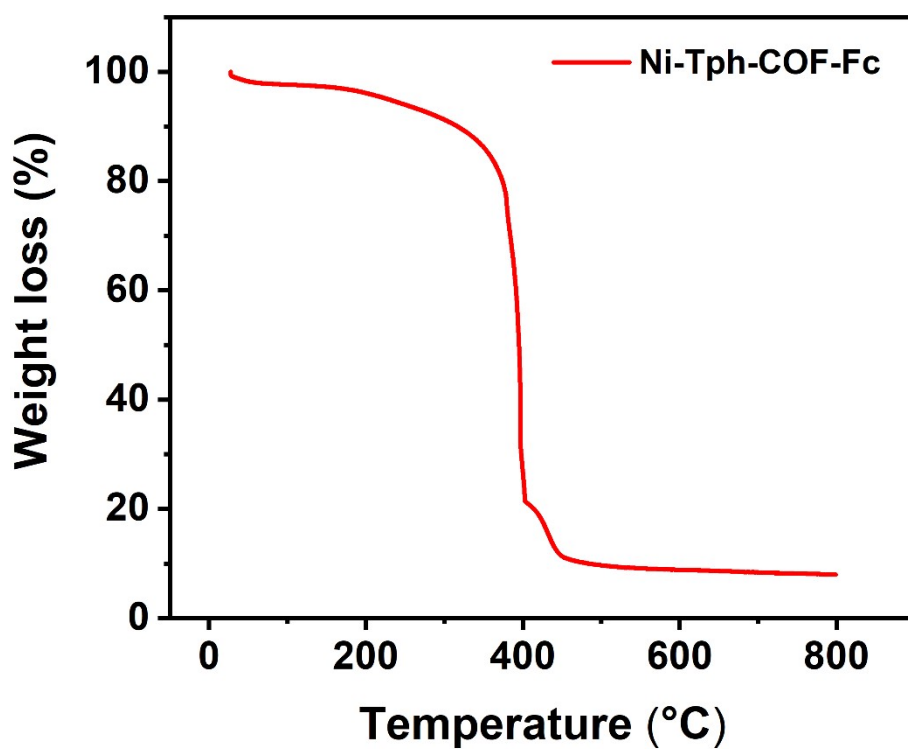
Fig. S10 TGA curve of Ni-Tph-COF-Fc under air atmosphere.
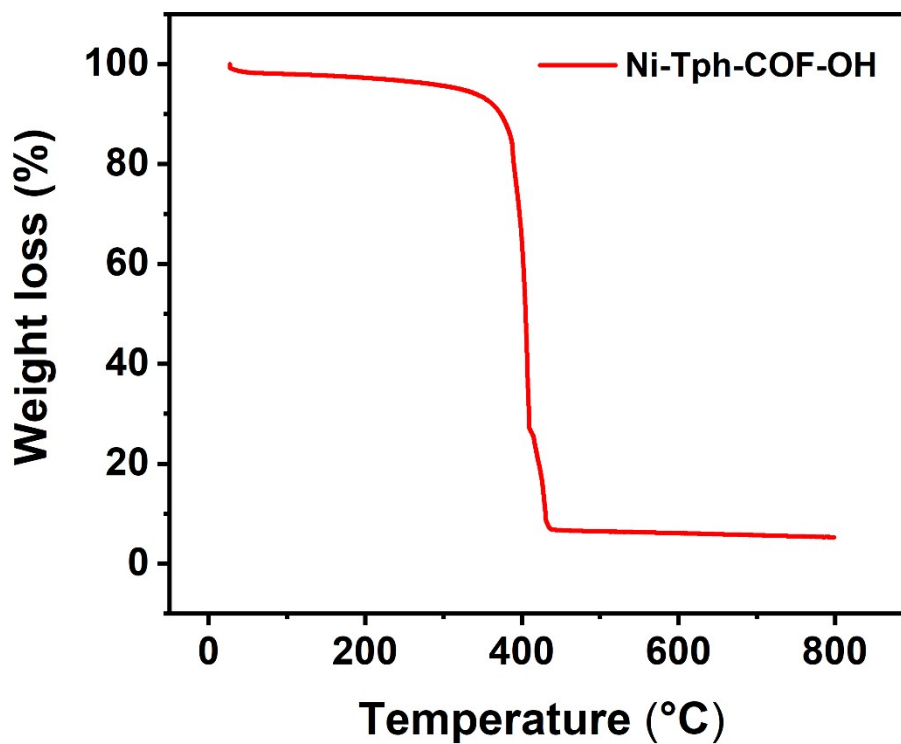
Fig. S11 TGA curve of Ni-Tph-COF-OH under air atmosphere.
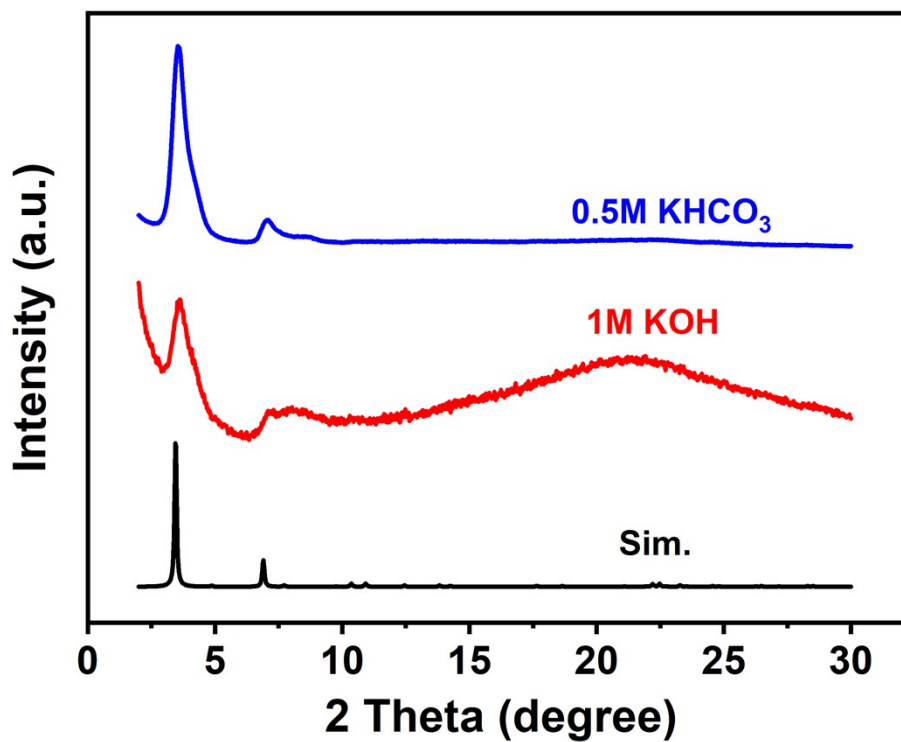
Fig. S12 The PXRD patterns of Ni-Tph-COF-OH after soaking in 1 M KOH and 0.5 M KHCO$_3$ aqueous solutions for 12 hours.
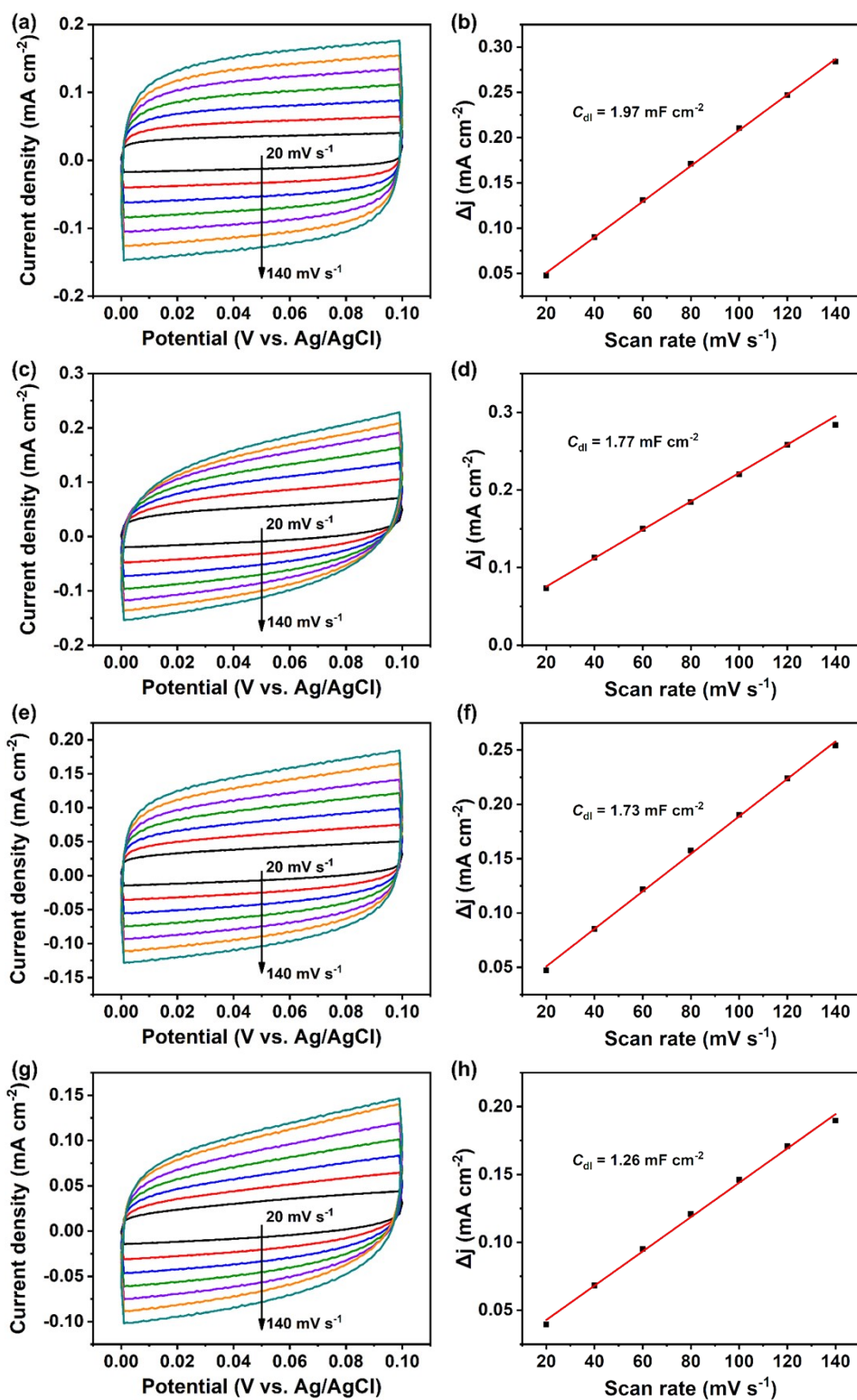
Fig. S13 The C_{dl} of different catalysts. (a, c, e, g) The CV plots of Ni-Tph-COF-Fc, Ni-Tph-COF-OH, Tph-COF-Fc, and Tph-COF-OH, with rates ranging from 20 to 140 mV s^{-1}, respectively. (b, d, f, h) The C_{dl} of Ni-Tph-COF-Fc, Ni-Tph-COF-OH, Tph-COF-Fc, and Tph-COF-OH, respectively.
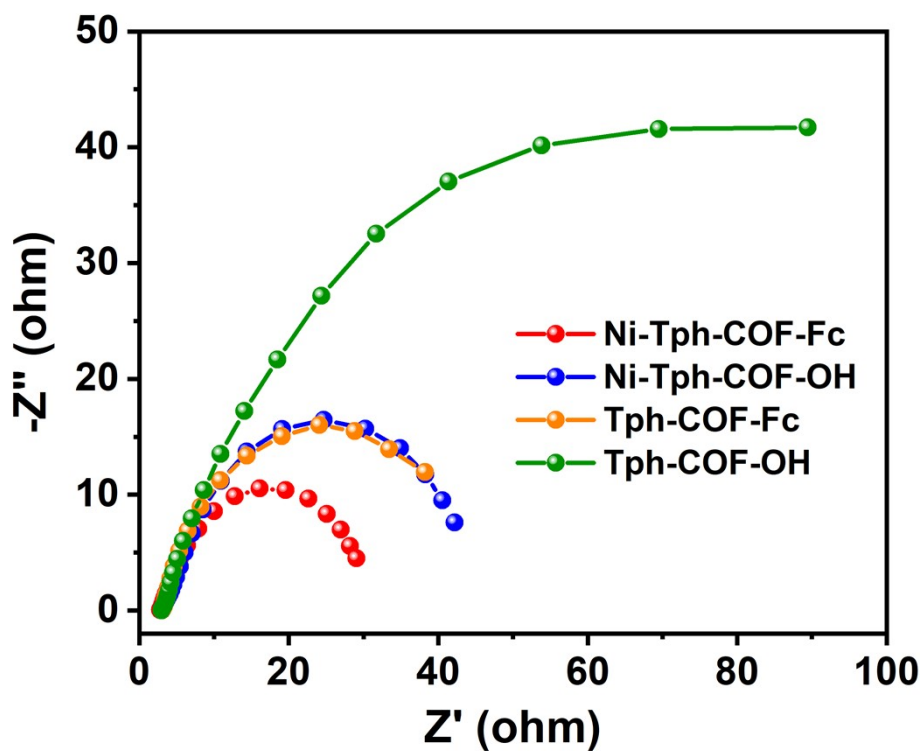
Fig. S14 The electrochemical impedance spectra of Ni-Tph-COF-Fc, Ni-Tph-COF-OH, Tph-COF-Fc and Tph-COF-OH.
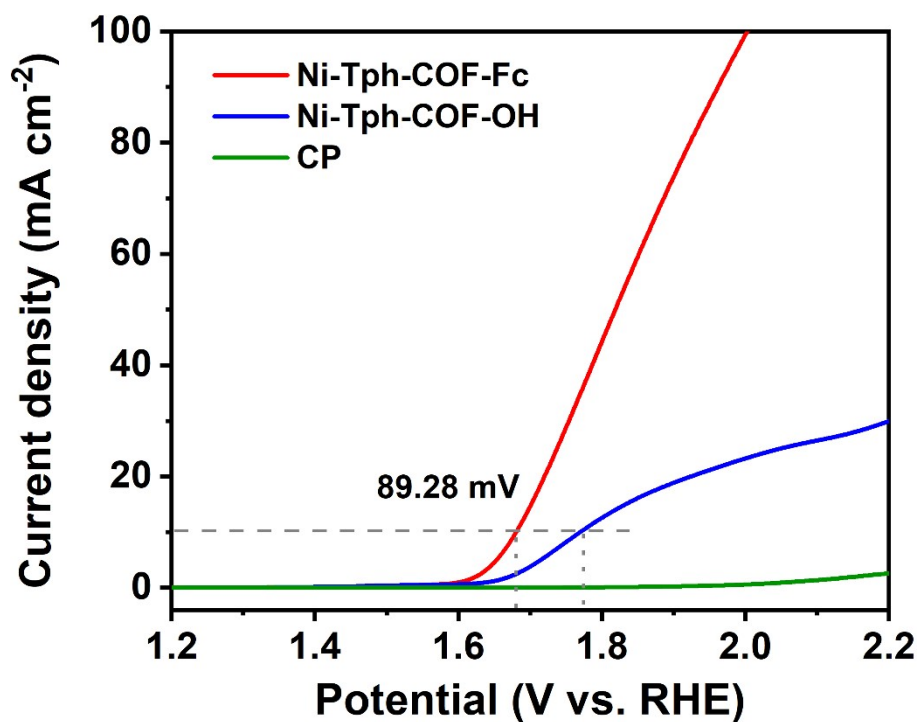
Fig. S15 LSV of Ni-Tph-COF-Fc, Ni-Tph-COF-OH and CP loading with AB and Nafion.
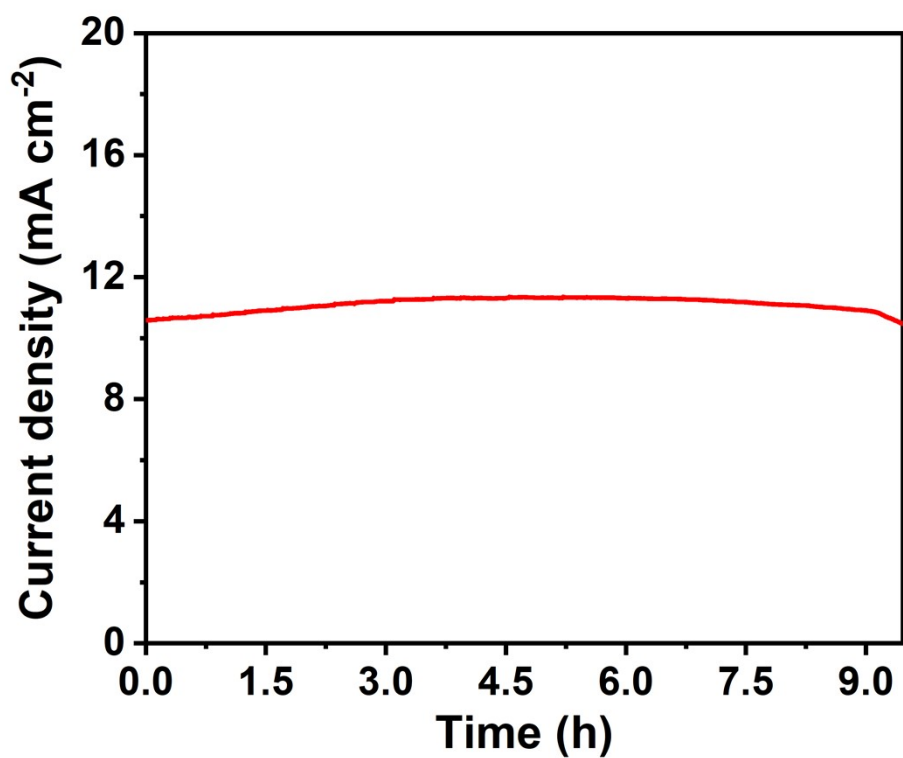
Fig. S16 The stability of Ni-Tph-COF-Fc for OER.
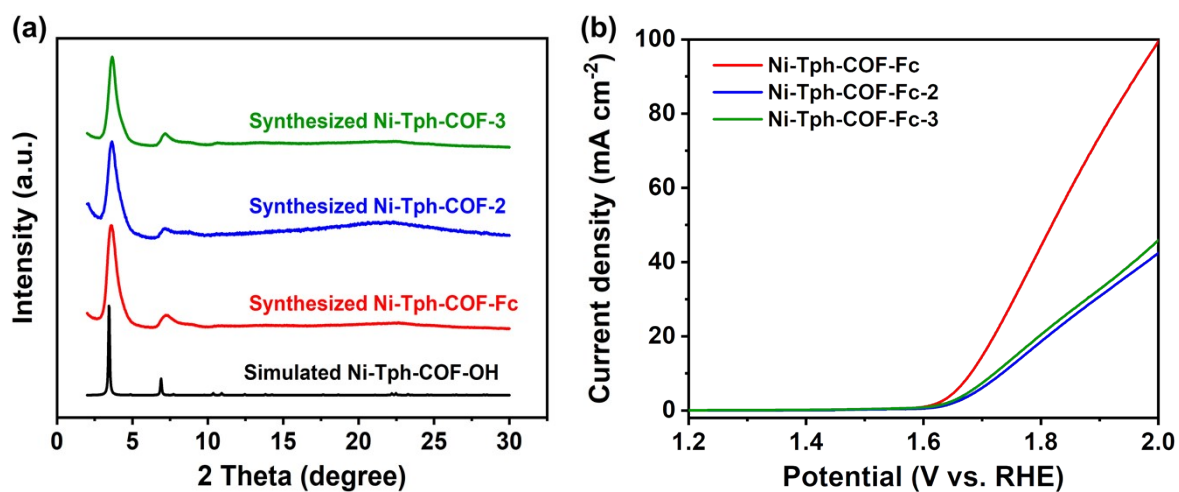
Fig. S17 (a) The PXRD patterns of Ni-Tph-COF-Fc-2 and Ni-Tph-COF-Fc-3. (b) LSVs of Ni-Tph-COF-Fc, Ni-Tph-COF-2 and Ni-Tph-COF-2.
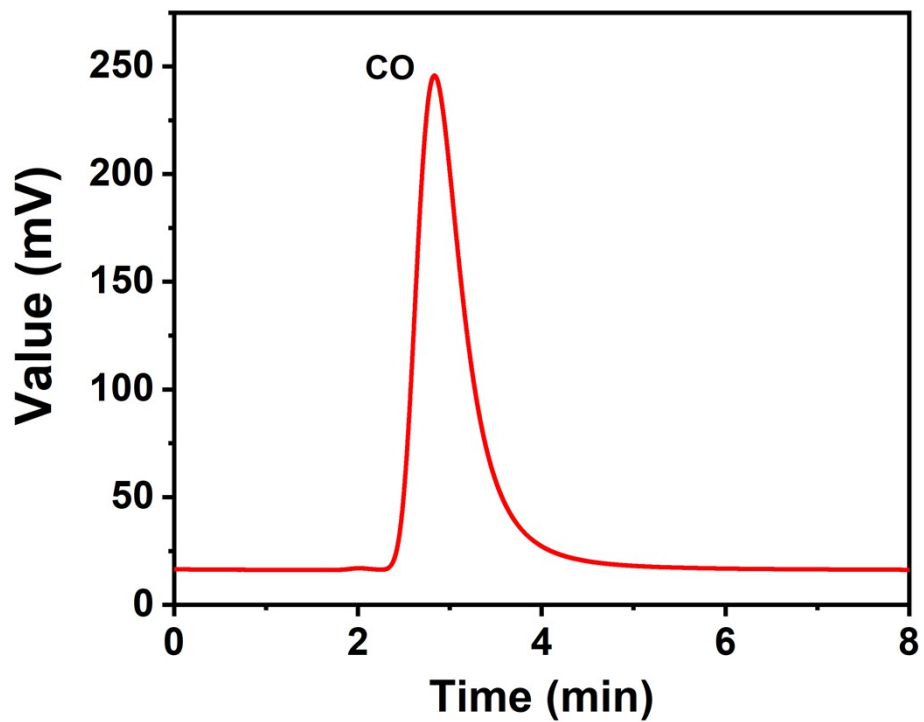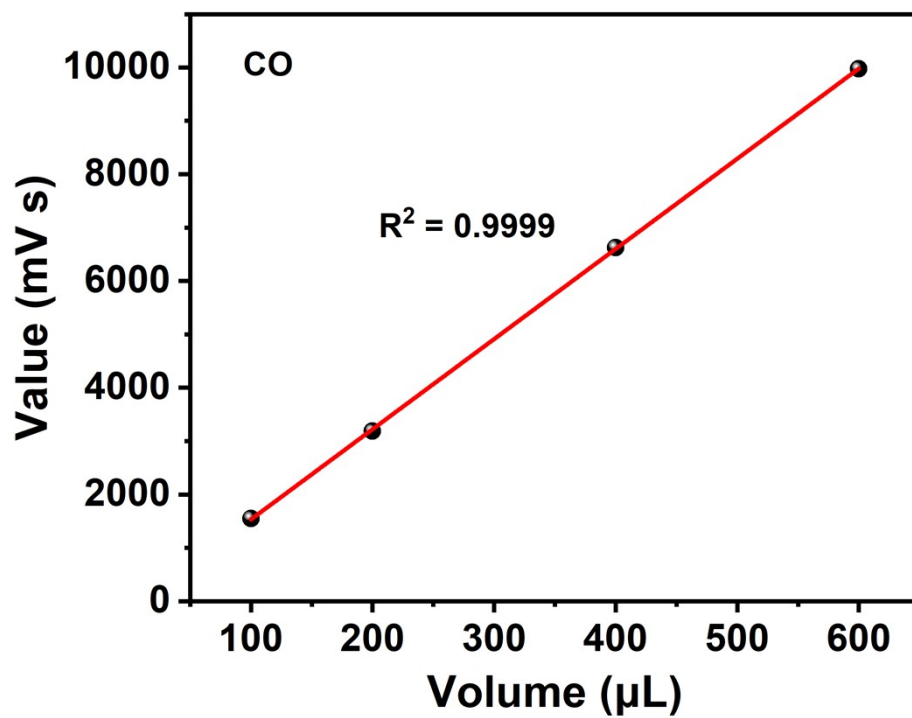
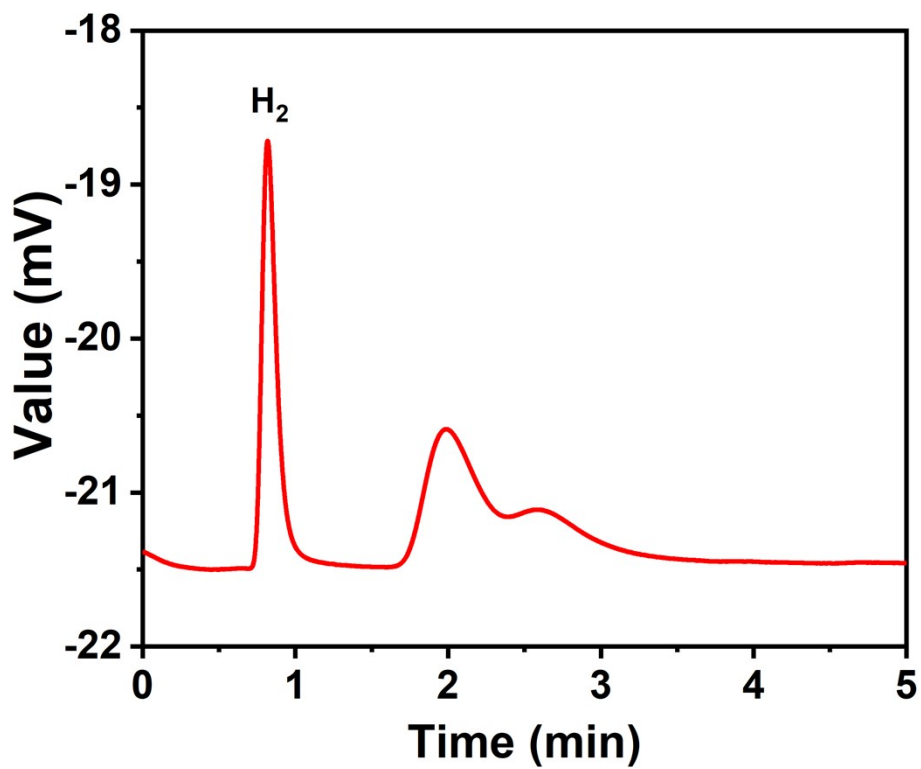**Fig. S18** Gas chromatogram of CO.

Fig. S19 Standard curve of CO.

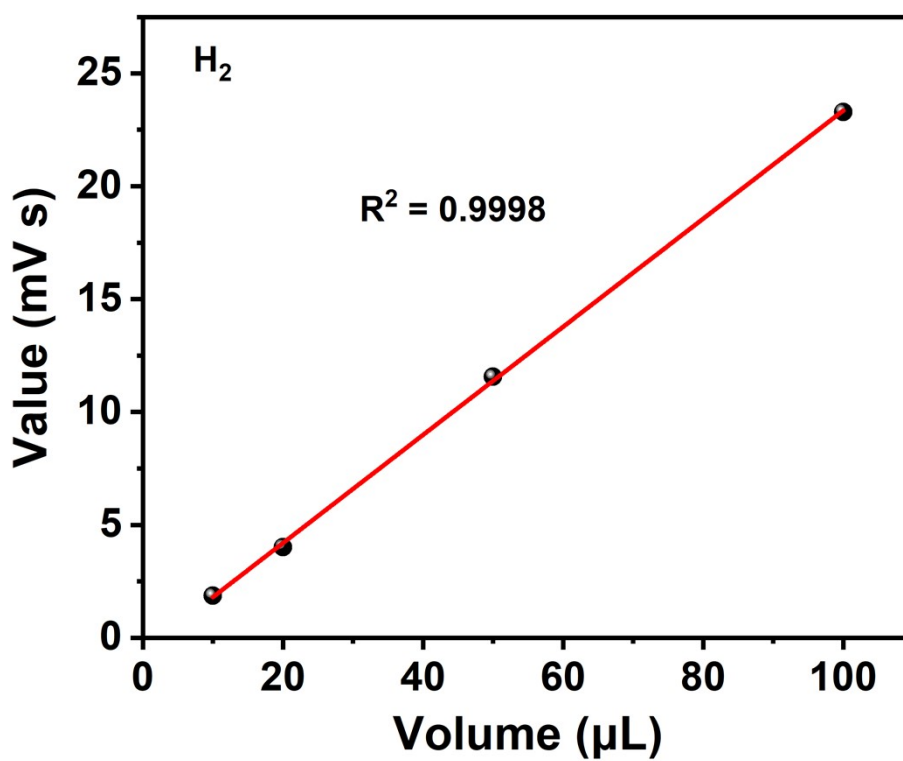**Fig. S20** Gas chromatogram of H_2.

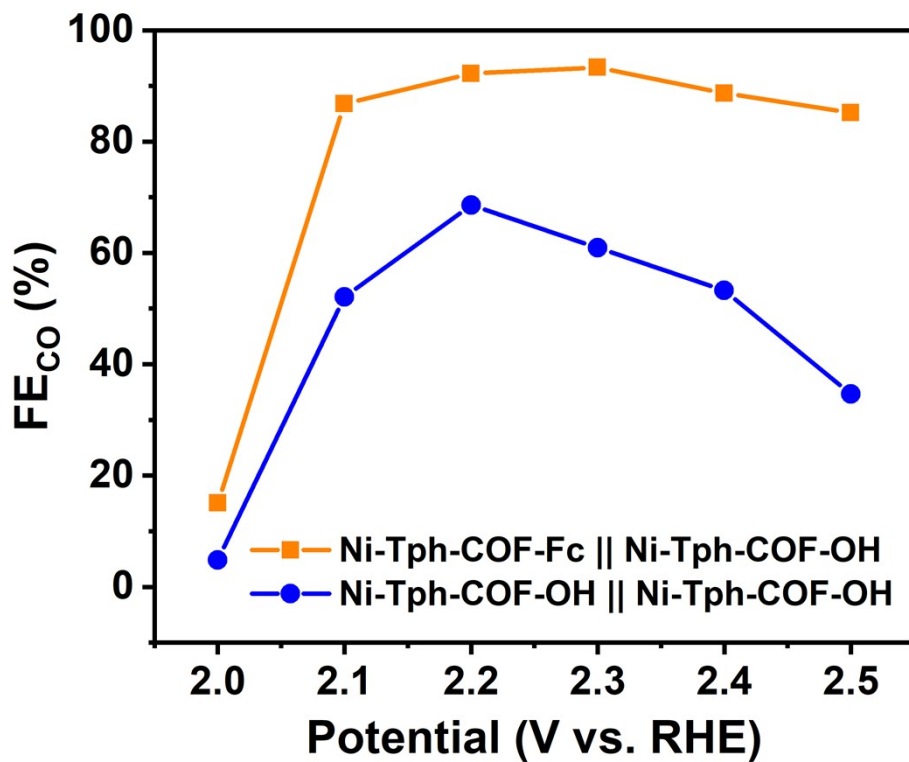**Fig. S21** Standard curve of H_2.

Fig. S22 The CO_2RR performance in a two-electrode system.
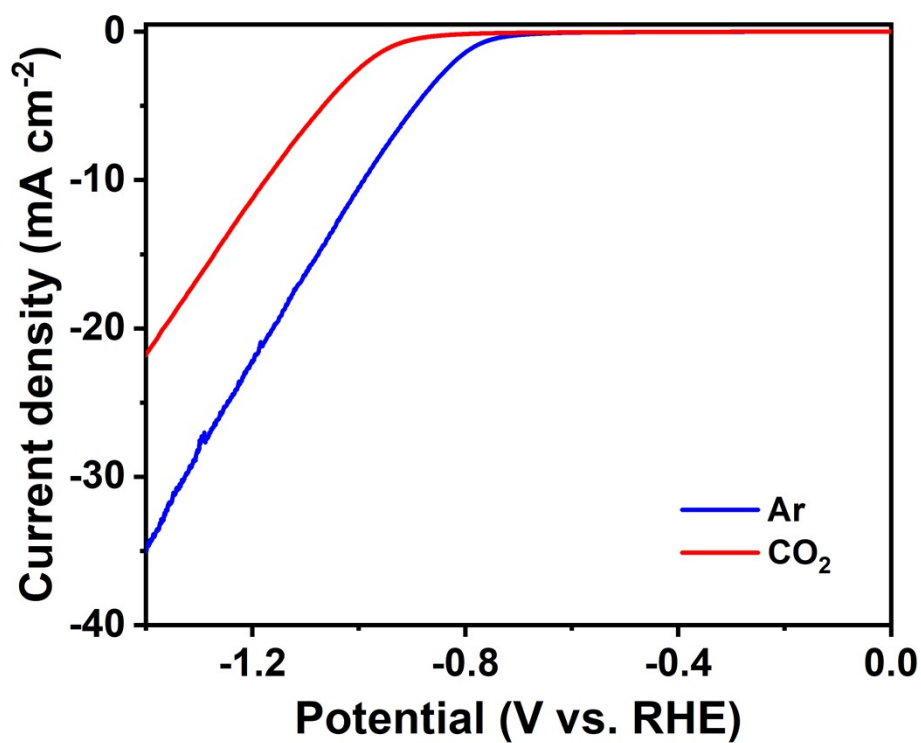
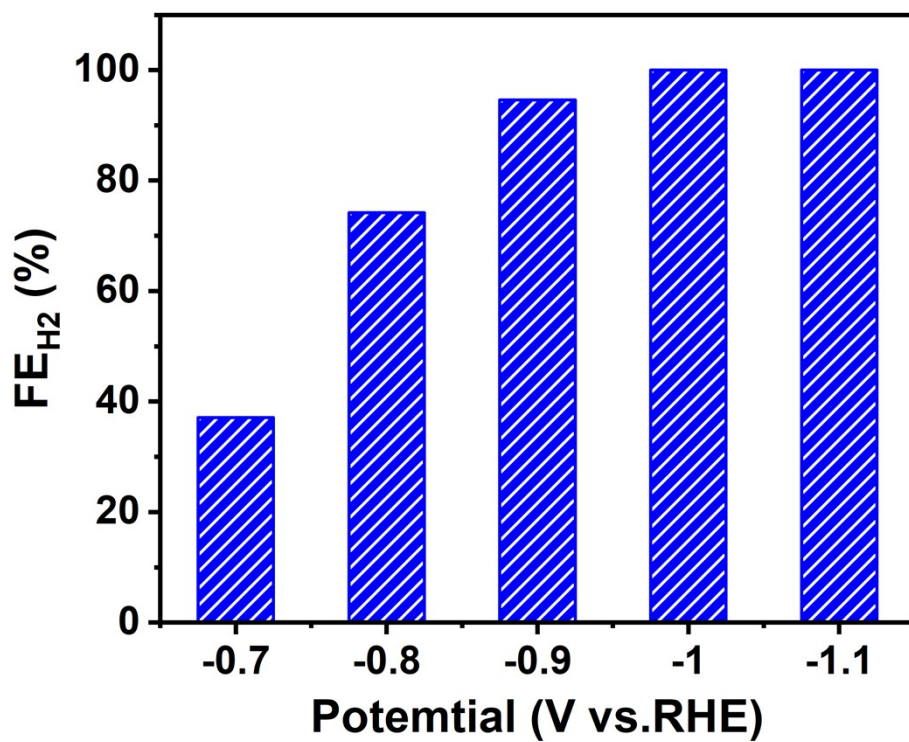**Fig. S23** The LSV curves of CO_2RR for CP under Ar or CO_2 atmosphere.

Fig. S24 The FE_{H2} of CO_2RR for CP laoding with AB and Nafion.